Hindawi
Wireless Communications and Mobile Computing
Volume 2023, Article ID 9823659, 1 page
https://doi.org/10.1155/2023/9823659

Retraction

Retracted: Wireless Control Industrial Robot Processing Irradiation System Based on Artificial Intelligence Technology

Wireless Communications and Mobile Computing

Received 18 July 2023; Accepted 18 July 2023; Published 19 July 2023

This article has been retracted by Hindawi following an investigation undertaken by the publisher [1]. This investigation has uncovered evidence of one or more of the following indicators of systematic manipulation of the publication process:

(1) Discrepancies in scope
(2) Discrepancies in the description of the research reported
(3) Discrepancies between the availability of data and the research described
(4) Inappropriate citations
(5) Incoherent, meaningless and/or irrelevant content included in the article
(6) Peer-review manipulation

The presence of these indicators undermines our confidence in the integrity of the article's content and we cannot, therefore, vouch for its reliability. Please note that this notice is intended solely to alert readers that the content of this article is unreliable. We have not investigated whether authors were aware of or involved in the systematic manipulation of the publication process.

Wiley and Hindawi regrets that the usual quality checks did not identify these issues before publication and have since put additional measures in place to safeguard research integrity.

We wish to credit our own Research Integrity and Research Publishing teams and anonymous and named external researchers and research integrity experts for contributing to this investigation.

The corresponding author, as the representative of all authors, has been given the opportunity to register their agreement or disagreement to this retraction. We have kept a record of any response received.

References

[1] L. Zhao, Q. Li, and G. Ding, "Wireless Control Industrial Robot Processing Irradiation System Based on Artificial Intelligence Technology," *Wireless Communications and Mobile Computing*, vol. 2022, Article ID 7068596, 8 pages, 2022.

Hindawi
Wireless Communications and Mobile Computing
Volume 2022, Article ID 7068596, 8 pages
https://doi.org/10.1155/2022/7068596

Research Article

Wireless Control Industrial Robot Processing Irradiation System Based on Artificial Intelligence Technology

Lijun Zhao,[1] Qingsheng Li ,[2] and Guanhua Ding[3]

[1]*Electrical and Electronic Engineering Department, Hebei Petroleum University of Technology, Chengde 067000, China*
[2]*Security Division, Hebei Petroleum University of Technology, Chengde 067000, China*
[3]*School of Electronic and Information Engineering, Beihang University, Beijing 100191, China*

Correspondence should be addressed to Qingsheng Li; liqingsheng@cdpc.edu.cn

Received 17 February 2022; Revised 16 March 2022; Accepted 1 April 2022; Published 9 May 2022

Academic Editor: Junjuan Xia

Radiation processing technology has been more and more widely used in light industry, chemical industry, food preservation, medical care, and other industries. Therefore, this paper designs a kind of wireless control system based on artificial intelligence technology γ radiation method, to strengthen the application of radiation processing equipment, and γ radiation monitoring can strengthen the radiation monitoring of its surrounding environment. The experimental results show that the C/Si atomic ratio of oxidized SiC fiber in air treated by this scheme is about 1.75, while the C/Si atomic ratio of SiC(Be) fiber treated by electron irradiation is close to 1 : 1.

1. Introduction

Food irradiation, with its unique technical advantages to reduce the loss of agricultural products and food, improves food quality, control food-borne diseases, etc., gained more and more attention from countries around the world. According to the statistical report published by the Food and Agriculture Organization (FAO) of the United Nations, the International Atomic Energy Agency (IAEA), and the World Health Organization (WHO), more than 40 countries around the world have approved more than 200 kinds of irradiated food, the total annual market sales amounted to about 400,000 tons, and food irradiation processing has been recommended by FAO, IAEA, and WHO as an international key promotion project [1, 2]. Food irradiation processing with radiation sources mainly γ-ray, electron beam two major types, of which China's cobalt source γ-ray is more widely used. But with the electron gas pedal beam energy and beam under the device to improve and perfect, electron beam irradiation in the processing capacity and economic efficiency has shown increasing advantages and in recent years has become the core equipment of the new irradiation processing device. Statistics from the irradiation industry associations show that China has built power 5 KW and above radiation processing with 83 electron gas pedals, with a total power of nearly 6469 KW, and another 8 high-power electron gas pedal device is under construction. Because the gas pedal has a high degree of automation, it can realize the online production and no radioactive waste sources generated and other advantages, while the electron beam energy can be adjusted through the acceleration voltage, the system is more convenient to control, and the line volume is flat, the product absorbed dose in uniform. Therefore, electron beam irradiation is expected to become the development direction of food irradiation processing [3]. The country in the "thirteenth five-year plan" period will increase the electron beam irradiation food application research support, the national development and reform commission also has to nonnuclear

power application as an opportunity to the electron beam radiation application of industrialization has given support. However, at present, most of the research results of food irradiation in China are concentrated in the processing application field of cobalt source γ-rays, and the basic research and application development of electron beam food irradiation are still quite weak, so the authors intend to make a review on the current research status and application characteristics of electron beam food irradiation in this field at home and abroad, in order to play a brick to lead the jade effect and promote the application of domestic electron beam food irradiation [4, 5]. The development of electron beam food irradiation applications in China is expected.

Electron beam irradiation has the following characteristics and advantages: (1) The equipment operation is highly controllable. The electron beam is generated by the electron gas pedal, its generation and disappearance is controlled by the power switch of the gas pedal, the size of the ionizing radiation energy is also adjusted by the accelerating voltage of the gas pedal, and the system control is relatively convenient. The electron beam energy is continuously adjustable within a certain range, the line volume is flat, and most of the devices under the beam use transmission devices, so that the absorbed dose of the product is uniform [6].

The accelerator is also equipped with ozone catalyst treatment device to achieve zero external ozone emission. Accelerator power that cut off the radiation source is safe and reliable and has no radioactive waste sources [7, 8].

The contributions of this paper are as follows:

The effect of traditional chemical fumigation insecticides on killing insect eggs is poor. Therefore, through appropriate dose of electron beam irradiation, this paper can not only kill 100% of insectivores and edible fungi but also kill other insect eggs in food and forest, which has the ability of killing in the whole period.

In order to make irradiation sterilization thorough and effective, we have designed a sterilization scheme for low-density food or food surface, which adopts electron beam sterilization. Irradiation does not need to remove product packaging, has no secondary pollution, has little impact on food quality and nutrition, and has good environmental protection performance.

This experiment shows that this scheme can effectively degrade the residues of pesticides and veterinary drugs, which is conducive to food safety.

2. Related Work

Research shows that E-beam food irradiation has unique technical characteristics and advantages in solving food safety problems, especially in preventing foodborne pathogenic microbial contamination in food, and in import and export quarantine, there is great potential for application [9, 10]. Due to the unique physical state and quality characteristics of cold and fresh animal-derived foods, the commonly used sterilization methods such as high-temperature and high-pressure sterilization and pasteurization can no longer help, while electron beam irradiation treatment is currently a better technology for sterilizing and preserving cold and fresh foods. [11] reported that the use of electron beam 0-3.85 kGy irradiation of boneless pork can effectively kill Escherichia coli and Salmonella in cold meat. Meanwhile, the quality and taste of carton packaged products after electron beam irradiation were not affected when stored under frozen or refrigerated conditions, but longer storage would affect the product gloss [12]. In [13], small packages of fresh pork were irradiated with 1 kGy low-dose electron beam, and the pork samples were inoculated with 103-104 g of Salmonella before irradiation, and the package gases were air vacuumed with 25% CO_2, 50% CO_2, and 72% CO_2 [14]. Electron beam irradiation of minced pork infected with four viruses was found to completely inactivate the viruses at 4.4-5.24 kGy. [15] studied the irradiation effect of electron beam irradiation on Listeria monocytogenes in minced pork and found that the sensitivity of each strain to electron beam varied and the sterilization D10 dose ranged from 0.372 to 0.447 kGy, for which he suggested the process dose of electron beam sterilization to be 4.5 kGy. [16] treated marinated chicken breast with electron beam and stored at 2°C for 8 weeks after irradiation at 2.9 kGy, the microbiological indexes met the requirements and had no effect on the quality. studied the resistance of a fungal spore to γ-rays and electron beam irradiation and showed that the sterilization effect of both was basically similar at the same absorbed dose. For the study of electron beam sterilization and preservation of cold and fresh animal-derived foods, scholars at home and abroad have also made useful exploration. For example, [5] investigated the effect of electron beam irradiation on the survival and repair of Escherichia coli at different pH. Blank et al. studied the sterilization effect of electron beam irradiation on cheese. [6] studied the effect of electron beam on the physical, physicochemical, and functional parameters of frozen stored liquid egg yolk [8–10].

E-beam irradiation has shown unique technical advantages and significant effects in killing microorganisms and pathogenic bacterial contamination in foods of plant origin. [7] used 10 kGy E-beam to irradiate eight spices, such as black pepper, onion powder, garlic powder, and white pepper, all of which were able to reduce the total bacterial content to less than 100 g without any significant effect on the quality. [8] studied wheat inoculated with spores of two strains of Tilletia controversa and T. tritici by 0-10.2 kGy E-beam irradiation, and the former bacteria were completely killed at a dose of 4.6-4.7 kGy. The doses of 4.6-4.7 kGy for the former strain and 10.2 kGy for the latter strain showed that a higher killing dose was required to kill the fungal spores as in the case of γ-rays. Studies on the processing quality of irradiated wheat showed that the E-beam irradiation treatment had no significant effect on its nutritional quality and processing characteristics, except for the reduction of surface gloss and water absorption of wheat. [9] irradiated brown rice, wheat, and mangold with E-beam and found that the total number of bacteria decreased to less than 100 g at 4 kGy irradiation and its viscosity was not affected, nor did it cause degradation of starch [10].

The above study shows that although the study of the effect of electron beam irradiation is not enough compared

with the study of the effect of γ-ray irradiation in terms of scope and depth, but it has a very good effect on foodborne microbial contamination and pathogenic bacteria, is an effective technical means to ensure food quality and safety, and in the dose range used has little effect on food quality and processing characteristics.

3. High-Energy Electron Accelerator

There are two main types of electron gas pedals used for irradiation processing, namely, electron linear gas pedals and high-voltage electron gas pedals, most of the irradiation gas pedals in the past belong to high-frequency, high-pressure type gas pedals, energy is mostly below 5 Mev. At present, directly used for irradiation of food, drugs, and medical devices, high-energy gas pedals are mainly microwave linear gas pedal and Loder gas pedal, the maximum output power of linear gas pedal has reached 15~25 kW, output/input ratio of about 10% to 20%. Most of the high-energy gas pedals produced in China are linear accelerators [15].

Therefore, these three types of gas pedals have their advantages and disadvantages, the structure of the standing wave gas pedal is the simplest and the smallest, and the return gas pedal is the second; the traveling wave and return gas pedal maximum beam power is relatively large and the standing wave gas pedal is slightly smaller; efficiency, the return gas pedal has the highest overall efficiency, small size, and simple structure, but the development time is short, and the application is just starting [5]. Therefore, in practical applications, the appropriate type can be selected according to its characteristics.

Russia, Japan, Belgium, France, and other countries are able to produce high-energy electron gas pedals [6]. Among them, Belgium IBA company strength is the strongest and its production of RHODOTRON type gas pedal high energy (10 MeV), high power, and advanced technology in the gas pedal for irradiated food and radiation disinfection in the world is leading.

In recent years, the domestic gas pedal research and development work is progressing rapidly, and on December 18, 2007, by the China Atomic Energy Research Institute of independent design and development of high-energy, high-power electron irradiation gas pedal 10 MeV/15 kW electron gas pedal irradiation demonstration project formally passed the acceptance [8].

4. Protection Requirements for Hardware Facilities

4.1. Radiation Safety Control Measures for Gamma Irradiation Processing Devices. Industrial γ-irradiated processing devices are used to irradiate products through γ-rays emitted by the decay of radionuclides to achieve certain purposes. At present, the γ sources of irradiators used in industry are mainly the nuclides 60Co, 137Cs, and so on. In the γ source used in industry, the γ source must be well controlled for protection. Before using γ source for industrial irradiation, the activity of γ source should be measured and calculated, and the correct safety measures should be taken according to the activity of the source. In the process of using γ source to irradiate industrial products, the source takes shielding measures in the process of using γ source to irradiate industrial products [5]. The open pool around the physical isolation must be set up (maintenance or auxiliary operations can be removed) to prevent the personnel concerned from inadvertently falling into the pool [6]. In the industrial irradiation of γ sources to reach the service life, to be replaced γ sources, and the decommissioning of γ sources for certain treatment. At present, the management of retired sources is confusing, for the end-of-life sources do not know how to deal with disposal caused a number of unused sources or waste sources out of control accidents [7]. To extend the service life of the source, it is necessary to submit to the audit and control department to check the sealing of the source, and only after passing can be used. Decommissioned sources can be returned to the business or disposed of as radioactive waste.

4.2. Radiation Safety Control Measures for Irradiation Sites. Irradiation sites are generally divided into control areas and supervision areas [8]. Control area is under normal conditions to control normal exposure or to prevent the spread of contamination, to prevent potential exposure type, to limit its extent, and to take special protective measures' type to make safety provisions of the area, not designated as a control area for the supervision of the area [5]. In the control area of the import and export, radiation danger warning signs must be set up, industrial irradiation γ sources used in the control area. In order to reduce the impact of direct and scattered radiation on the workplace outside the radiation room, the γ source storage channels to be labyrinthine and pays attention to ventilation. The air in the irradiation room irradiated by the strong source produces small amounts of harmful gases: ozone molecules and nitrogen oxides, where the amount of O_3 production is larger than that of NOx [9].

In order to prevent the effect of harmful gases on the staff, it is necessary to take good ventilation measures and centrifugal fans for air extraction. Means must be provided in the irradiation room and on the control console to stop, quickly interrupt, or terminate the operation of the irradiator at any moment and return the source to a fully shielded state, and there must be alarms and safety features in the irradiation room that can give visual and audible alarms when the source is out of control [6, 10]. In addition, for the site selection of γ irradiation processing device, the site of γ irradiation processing device should be selected from a stable site with good geological conditions, avoiding high-voltage transmission corridors and flammable and explosive sites according to the relevant national norms, and meeting the requirements of relevant national standards in the seismic protection zone. Comprehensive from the above requirements, collect hydrological, geological, meteorological, demographic, geographic ring mirror, seismic, and other information after the ring mirror impact assessment and after the regulatory approval to determine the plant site [5].

5. Manufacturing Solutions for This Article

5.1. Raw Materials. The PBeCS pioneer filament was synthesized in the laboratory [9], with a number average molecular weight of 2473, a molecular weight distribution of 3.36, and a softening point of 197°C.

5.2. Experimental Method

5.2.1. Electron Beam Irradiation of PBeCS Pioneer Filaments without Melting Treatment. Weigh the PBeCS pioneer wire in a fixed container, first vacuum, to achieve the required target vacuum, to the container into the gas containing oxygen and nitrogen and then continue to pump the vacuum, repeated 3 to 5 times to achieve the purpose of changing out the gas. Then, the gas is introduced and the flow ratio of $N_2 : O_2$ is controlled as 200 : 1, start to turn on the electron gas pedal (3.5 MeV), ensure that the electron flow is 1.5 mA (the dose rate is 0.63 kGy/s), irradiate continuously to the required irradiation dose (1.0, 1.5, and 2.0 MGy), reach the required irradiation dose, then turn off the gas pedal, stop irradiation, then remove the sample, weigh the mass, and calculate the mass loss rate.

5.2.2. Preparation of SiC(Be) Fibers. The PBeCS pioneer wire was weighed, placed inside the crucible, pressed with graphite at both ends, placed in a high-temperature tube furnace, protected by inert gas, at 500°C (heating rate 4°C/min), reacted for 2 h, then continued to heat up to 1250°C, reacted for 1 h, and naturally cooled to room temperature to obtain black SiC fibers.

5.3. Analytical Testing

5.3.1. Infrared Absorption Spectra. After the irradiated samples were made into KBr compacts, the infrared absorption spectra were measured by a Nicolet 6700 smart FTIR spectrometer. A simple semiquantitative analysis was performed according to the Lambert-Beer law. The ratio of the absorbance of different absorption peaks can be reduced to

$$\frac{A_1}{A_2} = \frac{K_1}{K_2} \times \frac{C_1}{C_2} = K\frac{C_1}{C_2}. \quad (1)$$

In this work, the degree of cross-linking reaction can be determined semiquantitatively by the change of Si-H, assuming the characteristic peak at 1250 cm^{-1} of Si–CH_3 as the internal standard in the calculation of the oxidation of the precursor PCS protofilament:

$$P_{\mathrm{Si-H}} = \frac{(A_{2100}/A_{1250})_g - (A_{2100}/A_{1250})_o}{(A_{2100}/A_{1250})_g} \times 100\%, \quad (2)$$

where A_{1250} is Si–CH_3 absorption peak intensity at 1250 cm^{-1}.

A_{2100} is the absorption peak intensity of Si-H at 2100 cm^{-1}; the subscript g represents green fiber; and the subscript o represents oxidation fiber.

5.3.2. Gel Content. The gel content was extracted in a continuous cycle of 15 times in a Soxhlet extractor with xylene as the solvent, and the mass change rate before and after extraction was calculated.

5.3.3. Elemental Analysis. The oxygen content of the fibers was tested by a LECO-60 combined meter (N/O/H); the elemental distribution on the diameter of the silicon carbide fibers was analyzed by an auger electron spectroscopy (AES) instrument of PHI 700 nanoscanning Osher system.

5.3.4. Microscopic Morphology Analysis. D8Discover diffractometer was used to analyze the phase of SiC fiber crop, and JEM-2100F scanning electron microscope was used to observe the surface morphology of silicon carbide fiber.

5.3.5. Determination of Mechanical Properties. The tensile strength of the fibers was measured by Model-YG001B electronic fiber strength meter with a specimen distance of 25 mm and a tensile rate of 2 mm/min.

6. Results and Discussion

6.1. Effect of Electron Irradiation on the Chemical Structure of PBeCS Pioneer Filaments. The infrared spectra of PBeCS precursor wires before and after irradiation are shown in Figure 1.

The main characteristic peaks of the FTIR spectra of each PBeCS pioneer filament sample are as follows: 3450 cm^{-1} and 1650 cm^{-1} are the O-H vibrations in H_2O, probably caused by the moisture absorption of the pioneer filament; 2950 cm^{-1} and 2900 cm^{-1} are the C-H stretching vibrations of methyl(-CH_3) and methylene(-CH_2 -); 2100 cm^{-1} is the characteristic stretching vibrations of Si-H; 1410 $cm^{-1}$is the C-H deformation vibrations of Si- CH_3; and 1360 cm^{-1} are the C-H vibrations of Si-. The C-H stretching vibration peaks of methyl(-CH_3) and methylene (-CH_2) are 2950 cm^{-1} and 2900 cm^{-1}; 2100 cm^{-1} is the characteristic stretching vibration peak of Si-H; 1410 cm^{-1} is the C-H deformation vibration peak of Si-; and 1360 cm^{-1} is the C-H out-of-plane vibration peak of Si—CH_2—Si. C-H is the out-of-plane vibration peak; 1250 cm^{-1} is the Si-deformation vibration peak; 1020 cm^{-1} is the Si-C-Si stretching vibration peak on Si—CH_2—Si; and 820 cm^{-1} is the Si-C stretching vibration peak.

The Si-H bond is a very active functional group, which can promote the cross-linking of PBeCS precursor filaments by consuming itself and increase the yield of porcelainization. The relative amounts of the Si-H reactive groups were characterized by $A_{\mathrm{Si-H}}/A_{Si-CH_3}$, as shown in Table 1, and the ASi-H/ASi-CH_3 decreased gradually with the increase of irradiation dose. Combined with Figure 1, it can be seen that with the increase of irradiation dose, a gradually enhanced Si-OH characteristic vibration peak appeared at 3680 cm^{-1}, while a gradually enhanced C=O stretching vibration peak also appeared at 1710 cm^{-1}.

This is mainly caused by the reaction between the C-H side chain and oxygen to form C=O double bonds [1]; the absorption peaks in the range of 1000-1100 cm^{-1} have a tendency to enhance and broaden to higher wave numbers,

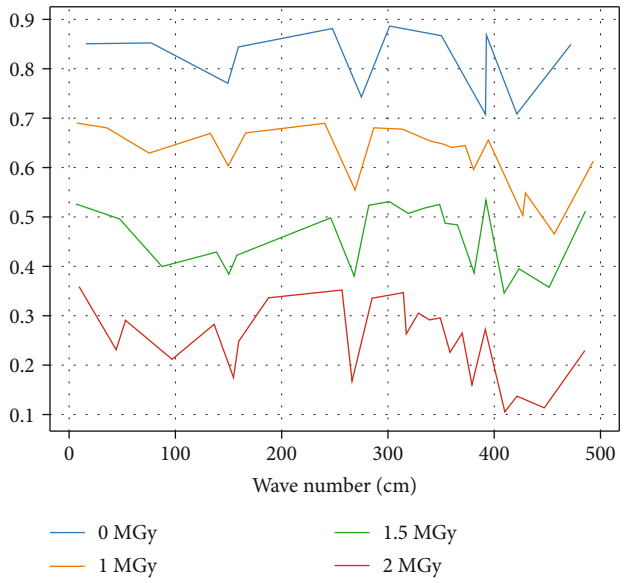

Figure 1: Infrared spectra of PBeCS pioneer filaments at different irradiation doses.

Table 1: Absorbance ratio of Si-H to Si-CH_3 in PBeCS pioneer filaments at different irradiation doses.

Irradiation dose/Mgy	A_{Si-H}/A_{Si-CH_3}
0	1.97
1	1.88
1.5	1.75
2	1.64

which is due to the close position of Si-O-Si and Si-CH_2-Si peaks, and appear to superimpose as one absorption peak, which also indicates the formation of Si-C-Si and Si-O-Si type bridging structures after irradiation.

6.2. Gel Content of Irradiated Products. During the cross-linking process of PBeCS pioneer filaments, the three-dimensional network structure begins to form, and the mass fraction of nonfusible material in the fiber, generally known as gel content, is mainly used to characterize the degree of nonfusion of the fiber [2], and the relationship between the gel content and oxygen content of PBeCS pioneer filaments and the irradiation dose is shown in Table 2. This indicates that the PBeCS precursor filaments do react with the oxygen in the mixed atmosphere under the electron beam irradiation, and the higher the irradiation dose, the higher the oxygen content.

When the irradiation dose was low, no gel content appeared, because only the oxidation reaction appeared and did not reach the irradiation dose required for the cross-linking reaction, with the dose further increased, the gel began to appear, and when the irradiation dose was 2.0 MGy, the gel content reached about 20%, and the fibers did not appear in the later sintering process, which indicates that after low dose irradiation by electron beam in oxygen-

Table 2: Effect of irradiation dose on PBeCS pioneer filaments.

Irradiation dose/ Mgy	Mass fraction of gel/%	Mass fraction of oxygen/%
0	0	0.76
1	0.1	3.54
1.5	0.7	4.98
2	19.8	5.97

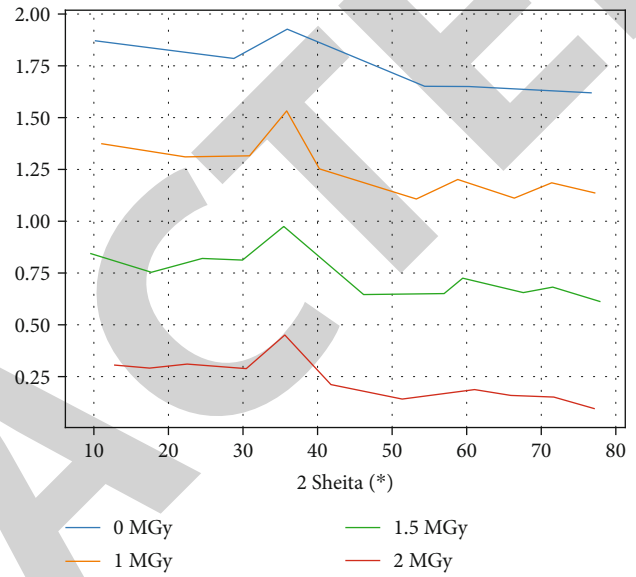

Figure 2: XRD patterns of beryllium-containing silicon carbide fibers with different irradiation doses.

containing atmosphere, it is possible to no melting treatment.

6.3. Microstructure and Mechanical Properties of SiC(Be) Fibers. The XRD patterns of the beryllium carbide containing fibers obtained by sintering the PBeCS pioneer filaments cross-linked with different irradiation doses at 1250°C under N_2 atmosphere are shown in Figure 2, where three sharp diffraction peaks, $\theta = 35.4°, 60.4°$, and $71.2°$, corresponding to the (111), (220), and (311) crystallographic planes of β-SiC, respectively, appear in the fiber diffraction patterns. 311) crystalline plane of β-SiC. From Figure 2, it can be seen that the intensity of the crystalline diffraction peak first increases with increasing irradiation dose and then tends to broaden and weaken. This is caused by the oxygen introduced during the irradiation process, which exists in the fiber as an amorphous phase SiC_xO_Y and its pyrolysis produces an amorphous SiO_2 that inhibits the grain growth. The higher the irradiation dose, the more oxygen is introduced, the more obvious the inhibition, and the worse the crystallinity.

When the PBeCS pioneer filaments treated with different irradiation doses were sintered under N_2 atmosphere, the crosslinking degree was too low at 1.0 and 1.5 MGy, and the merging of the silicon carbide fibers occurred as shown in Figure 3, and when the dose was continued to increase

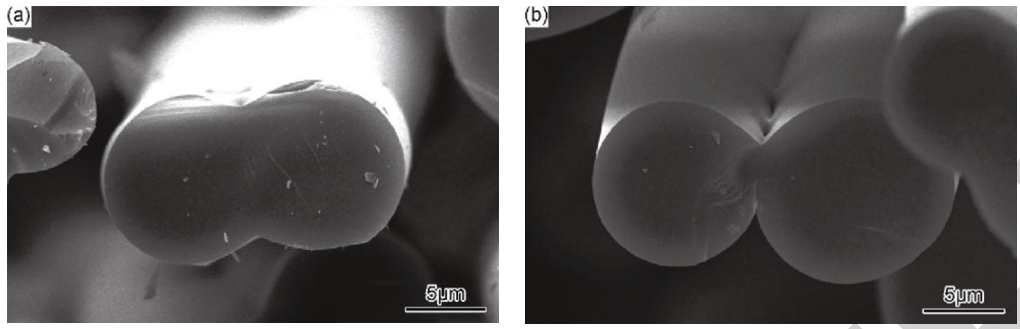

(a) (b)

Figure 3: SEM cross-sections of SiC(Be) fibers with different irradiation doses (a). 1.0 MGy. (b) 1.5 MGy.

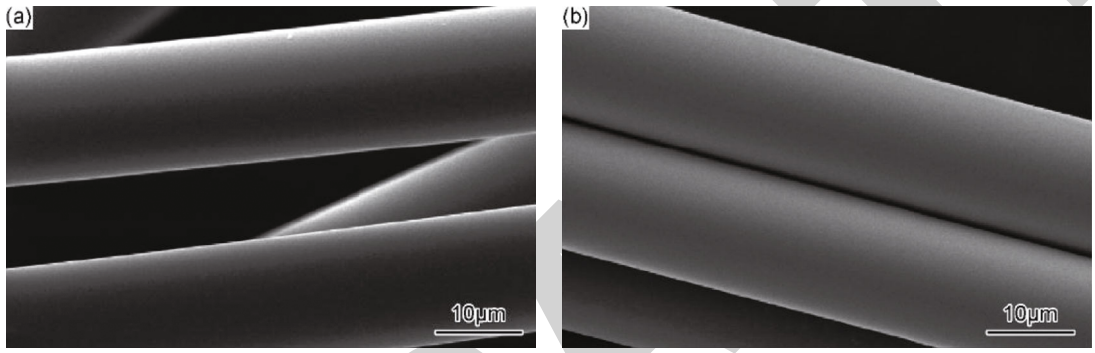

(a) (b)

Figure 4: SEM pictures of the surface of SiC(Be) fibers treated with air oxidation crosslinking and electron beam irradiation crosslinking. (a) Air oxidation crosslinking. (b) E-beam irradiation crosslinking.

Table 3: Mechanical properties of beryllium-containing silicon carbide fibers.

Curing method	Irradiation dose/Mgy	Tensile strength/Gpa	Tensile modulus/Gpa
Thermal oxidation curing in air	—	1.69	145
Electron beam irradiation	2	1.81	179

to 2.0 MGy, the gel content of the PBeCS pioneer filaments was relatively low (20%), but no merging occurred in the later sintering, and the synthesized fibers changed from the initial light yellow color to black as shown in Figure 4(b). The color of the synthesized fibers changed from light yellow to black at the beginning, as shown in Figure 4(b). The fibers cross-linked by irradiation at a dose of 2.0 MGy and air oxidation were tested for their mechanical properties, and the results are shown in Table 3, which shows that the strength of the fibers cross-linked by electron beam irradiation was significantly improved compared with those cross-linked by air oxidation.

Figure 4 shows the SEM photomicrographs of silicon carbide fibers cross-linked by air oxidation and irradiated at a dose of 2.0 MGy. From Figure 4, it can be found that the surface of the fibers was not damaged by the electron beam irradiation, and the fiber shape remained intact with a diameter of about 12-15 μm and a bright and dense surface. This further proves that electron beam irradiation has a good nonmelting effect on the pioneer filaments.

6.4. SiC(Be) Fiber Composition Analysis. The electron-irradiated and air-oxidized cross-linked fibers were sintered at 1250°C. The Si, C, and O content of the fibers was measured by AES (AES is difficult to test because the doped Be is a light element and its atomic fraction is less than 1%). As shown in Figures 5 and 6, the oxygen content of the electron irradiated fibers is 4.71% (atomic fraction, below), which is significantly lower than that of the air-oxidized cross-linked fibers (11.55%). The oxygen content of SiC fibers and its influence on the temperature resistance, creep resistance, and mechanical properties are important because the reaction of the oxygen-containing phase SiC_xO_Y in the fibers at high temperature results in the formation of SiO and CO gas, which leaves a large number of holes and defects in the fibers. This is because the reaction of the oxygen-containing phase 111 in the fiber at high temperature will form SiO and CO gas, which will leave a large number of holes and defects on the fiber, resulting in the destruction of the fiber structure and a rapid decrease in its tensile strength. At the same time, a large number of β-SiC

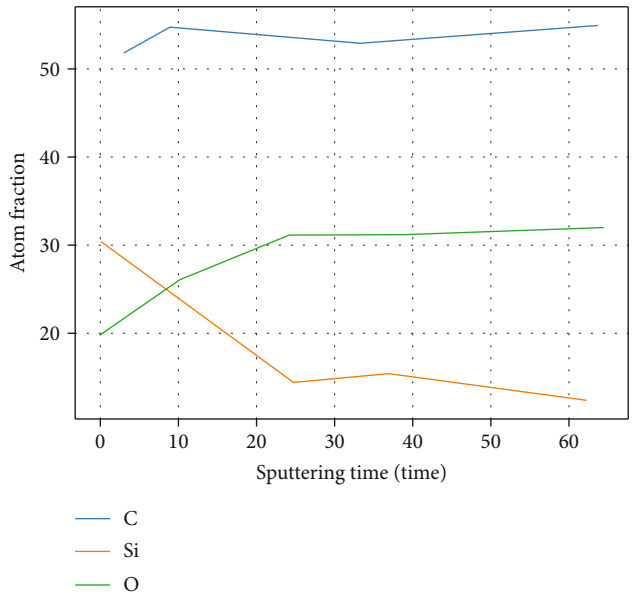

Figure 5: AES profile of SiC fibers cross-linked by air oxidation.

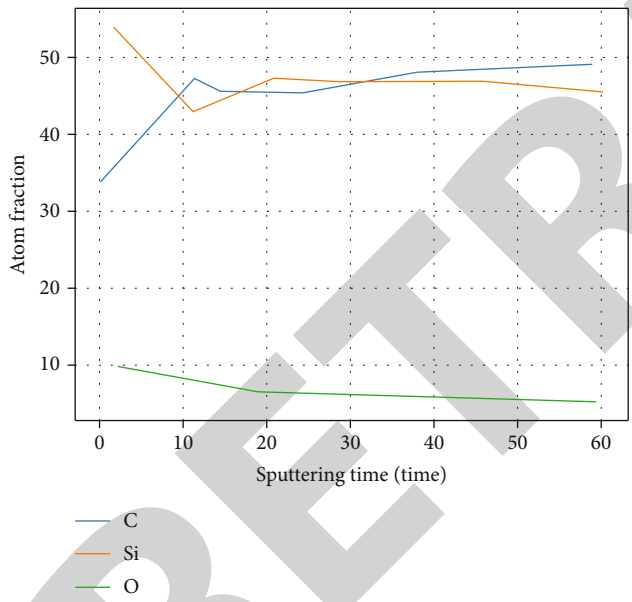

Figure 6: AES profile of electronically irradiated cross-linked SiC (Be) fibers.

microcrystals in the fiber are surrounded by SiC_xO_y, so that a large number of grain boundary phases will slip during the growth of fiber grains at high temperatures, resulting in lower creep resistance of the fiber [3, 4]. Therefore, reducing the oxygen content of fibers is a prerequisite for obtaining high-performance SiC fibers, and the use of electron irradiation crosslinking can significantly reduce the oxygen content of SiC fibers.

In addition, the C/Si atomic ratio of SiC fibers oxidized in air is about 1.75, while the C/Si ratio of SiC(Be) fibers treated by electron irradiation is close to the stoichiometric ratio of 1 : 1. For SiC fibers, the C/Si atomic ratio is another important index affecting their oxidation resistance, creep resistance, and mechanical properties. In SiC fibers, the presence of a large amount of excess C, which is sensitive to oxidizing atmosphere, reduces the oxidation resistance of the fibers, especially at high temperatures where the excess C will continue to oxidize and larger holes will appear on the fiber surface, which will promote the diffusion to the interior of the fibers and drastically reduce the fiber strength [15]. In addition, the distribution of excess C around the SiC grains will also limit the growth of β-SiC grains, while the carbon layer between the grain boundaries will promote grain boundary slip, resulting in fibers with low creep resistance [16].

Table 4: Parameters of chemical bonds in PBeCS pioneer filaments.

Chemical bond	Bond length/nm	Bond energy/(kj/mol^{-1})
Si—C	0.188	242.7-334.7
Si—H	0.147	320
C-H	0.107	415

6.5. Reaction Mechanism Speculation. In the PBeCS pioneer filament structure, the main chemical bonds are Si-C, Si-H, and C-H bonds, and the bond lengths and bond energies of these bonds are shown in Table 4, and the bond energy of Si-C bonds varies from 242.7 to 334.7 kJ/mol. The bond energy of Si-C bond varies in the range of 242.7 to 334.7 kJ/mol, and its specific value is related to the chemical environment around the C atom.

When the PBeCS pioneer filament is irradiated by electron beam, the high-energy electrons interact with the PBeCS pioneer filament and transfer the energy of the electrons through elastic collisions, in which the bond energy of Si-H (320 kJ/mol) is lower than that of C-H (415 kJ/mol), it is known that the H atom of Si-H bond is more active and can if the absorbed energy is sufficient, it is possible to get rid of the bond and become reactive particles or Si radicals, which react with oxygen to form Si-OH, which then undergoes dehydration condensation reaction to form Si-O-Si, and at the same time, as the bond energy of Si-C bond energy varies in the range of 242.7 to 334.7 kJ/mol, if the chemical environment around the C atom changes so that the Si-C bond energy is lower than that of Si-H (320 kJ/mol), then the Si-C bond will break, forming Si-CH_2-Si radicals, and the Si radicals will cross-link with Si-CH_2- to form Si-CH_2-Si.

7. Conclusions

The PBeCS pioneer filaments are irradiated by electron beam during irradiation to obtain nonmelting products by undergoing a series of chemical transformations. Irradiation in a low-oxygen atmosphere is mainly Si-H; Si-CH_3 reacts with O_2 to form Si-OH and C=O structured molecules, and then, Si-OH undergoes dehydration condensation to form Si-O-Si. Si-H reacts with Si- to form Si-CH_2-Si, and this structure is transformed into SiC fiber skeleton structure in later sintering.

The beryllium-containing SiC fibers were prepared by electron beam irradiation of nonmelting PBeCS pioneer filaments, and the fibers had smooth surfaces, formed β-SiC crystalline forms, and the oxygen content of the fibers was less than 5%, the C/Si ratio was close to 1 : 1, the average strength of the fibers was 1.81 GPa, and the average elastic modulus was 179 GPa.

Data Availability

The experimental data used to support the findings of this study are available from the corresponding author upon request.

Conflicts of Interest

The authors declared that they have no conflicts of interest regarding this work.

References

[1] J. Sharpey-Schafer, "Laboratory portrait: iThemba Laboratory for Accelerator-Based Sciences," *Nuclear Physics News*, vol. 14, no. 1, pp. 5–13, 2004.

[2] Y. Gong, S. M. Hu, X. L. Yang et al., "Comparative study on degradation of ethylene-propylene rubber for nuclear cables from gamma and beta irradiation," *Polymer Testing*, vol. 60, pp. 102–109, 2017.

[3] Y. Gong, J. Tang, X. L. Yang et al., "Effect of irradiation dose rates on ethylene-propylene rubber for nuclear cables," *Applied Surface Science*, vol. 484, pp. 845–852, 2019.

[4] T. Bortfeld, "IMRT: a review and preview," *Physics in Medicine & Biology*, vol. 51, no. 13, pp. R363–R379, 2006.

[5] S. Yang, W. Min, J. Ghibaudo, and Y. F. Zhao, "Understanding the sustainability potential of part consolidation design supported by additive manufacturing," *Journal of Cleaner Production*, vol. 232, pp. 722–738, 2019.

[6] K. H. Johansson, M. Törngren, and L. Nielsen, "Vehicle applications of controller area network," in *Handbook of networked and embedded control systems (pp. 741-765)*, Birkhäuser Boston, 2005.

[7] G. Tsakanova, N. Babayan, E. Karalova et al., "Low-energy laser-driven ultrashort pulsed electron beam irradiation-induced immune response in rats," *International Journal of Molecular Sciences*, vol. 22, no. 21, p. 11525, 2021.

[8] J. C. Clements and H. L. Hunt, "Marine animal behaviour in a high CO_2 ocean," *Marine Ecology Progress Series*, vol. 536, pp. 259–279, 2015.

[9] R. P. Croll and A. J. Dickinson, "Form and function of the larval nervous system in molluscs," *Invertebrate Reproduction and Development*, vol. 46, no. 2-3, pp. 173–187, 2004.

[10] E. Kotsyuba, A. Kalachev, P. Kameneva, and V. Dyachuk, "Distribution of molecules related to neurotransmission in the nervous system of the mussel Crenomytilus grayanus," *Frontiers in Neuroanatomy*, vol. 14, p. 35, 2020.

[11] A. Kinjo, M. Sassa, T. Koito, M. Suzuki, and K. Inoue, "Functional characterization of the GABA transporter GAT-1 from the deep-sea mussel Bathymodiolus septemdierum," *Comparative Biochemistry and Physiology Part A: Molecular & Integrative Physiology*, vol. 227, pp. 1–7, 2019.

[12] J. C. Clements, M. M. Bishop, and H. L. Hunt, "Elevated temperature has adverse effects on GABA-mediated avoidance behaviour to sediment acidification in a wide-ranging marine bivalve," *Marine Biology*, vol. 164, no. 3, p. 56, 2017.

[13] T. Bollner, P. W. Beesley, and M. C. Thorndyke, "Distribution of GABA-like immunoreactivity during post-metamorphic development and regeneration of the central nervous system in the ascidian Ciona intestinalis," *Cell and Tissue Research*, vol. 272, no. 3, pp. 553–561, 1993.

[14] L. Vitellaro-Zuccarello, S. De Biasi, P. Bernardi, and A. Oggioní, "Distribution of serotonin-, gamma-aminobutyric acid- and substance P-like immunoreactivity in the central and peripheral nervous system of Mytilus galloprovincialis," *Tissue and Cell*, vol. 23, no. 2, pp. 261–270, 1991.

[15] P. An, Z. Wang, and C. Zhang, "Ensemble unsupervised autoencoders and Gaussian mixture model for cyberattack detection," *Information Processing & Management*, vol. 59, no. 2, p. 102844, 2022.

[16] L. Vitellaro-Zuccarello, S. De Biasi, and A. Amadeo, "Immunocytochemical demonstration of neurotransmitters in the nerve plexuses of the foot and the anterior byssus retractor muscle of the mussel, Mytilus galloprovincialis," *Cell and Tissue Research*, vol. 261, no. 3, pp. 467–476, 1990.